

Development and Implementation of Amide Proton Transfer Chemical Exchange Saturation Transfer in the Spinal Cord at 3T Using Lorentzian Difference Analysis

Samantha By^{1,2}, Alex K. Smith^{1,2}, Lindsey M. Dethrage², Adrienne N. Dula^{2,3}, Siddhama Pawate⁴, and Seth A. Smith^{2,3}

¹Department of Biomedical Engineering, Vanderbilt University, Nashville, TN, United States, ²Vanderbilt University Institute of Imaging Science, Vanderbilt University, Nashville, TN, United States, ³Department of Radiology and Radiological Sciences, Vanderbilt University, Nashville, TN, United States, ⁴Department of Neurology, Vanderbilt University, Nashville, TN, United States

Target Audience: Physician/scientists interested in CEST imaging, clinicians interested in quantitative spinal cord imaging

Purpose: Amide proton transfer (APT) chemical exchange saturation transfer (CEST) is a spectrally specific, low power magnetization transfer experiment that has recently gained significant interest due to its sensitivity to pH and protein concentration [1]. APT CEST is well suited to exploit direct chemical exchange between amide protons of the protein/peptide backbone in the spinal cord to potentially probe metabolic composition of spinal cord lesions in diseases such as multiple sclerosis (MS) and may be sensitive to such pathologies such as axonal congestion and protein accumulation in the earliest stages of lesion formation in MS. However, there are few reports of APT CEST in the spinal cord [2] and even fewer studies have applied the method to spinal cord diseased cohorts. Here, we investigate the application of a pulsed CEST acquisition with a Lorentzian difference analysis in healthy controls and 1 MS patient with known spinal cord lesions and clinical dysfunction related to spinal cord damage.

Methods: We have applied CEST in the cervical spinal cord of six healthy controls (3 males/3 females, mean age: 26 years old, range: 21-34) and 1 relapsing-remitting MS patient (female, 34-years-old). Imaging was acquired using a 3.0T whole body MR scanner (Philips Achieva, Best, Netherlands). A quadrature body coil was used for excitation and a 16-channel SENSE neurovascular coil (Nova Medical) was used for reception.

Data Acquisition: A high-resolution (0.6x0.6x5 mm³) multi-echo gradient echo (mFFE, [3]) anatomical image was acquired in the axial plane for co-registration (TR/TE/ATE = 700/7.2/8.8 ms, $\alpha = 28^\circ$) and lesion detection. For CEST, a 3D multi-shot, EPI (EPI factor=5, SENSE factor RL=1.5), fast field echo (20° flip angle, TR/TE=155/7.9ms) was used to acquire 14 slices with resolution of 1x1x5mm³ and FOV of 160mm x 160mm, which covered the cervical spinal cord from approximately C2-C7. The CEST spectra with a binomial excitation (fat suppression, ProSet 1-3-3-1 pulse) were acquired using a 2 μ T pulse, 75 ms RF Gaussian prepulse at 37 asymmetrically sampled offsets between ± 4.5 ppm. Total scan duration was 13:49 minutes.

Data Processing: CEST data was rigidly registered to the anatomical mFFE slice by slice using the FLIRT package from FSL (FMRIB, Oxford, UK). Data was analyzed using a base-line drift correction to correct temporal fluctuations in CEST acquisition similarly to [4]. Additionally, we corrected for B_0 inhomogeneity by fitting the CEST spectra to a single Lorentzian curve with a baseline, which is further modified with a maximum-signal intensity correction term to account for data points with low signal-to-noise ratio (SNR) at the extremity of the spectra on a voxel-by-voxel basis. This ensures that the Lorentzian fit is “tacked” to the maximum value of the z-spectrum. The APT CEST effect was then calculated using a voxel-wise analysis as the integrated area between the fitted Lorentzian curve and the acquired CEST spectra (residual) from 3-4ppm [5]. Lastly, ROIs on a lateral column, dorsal column, gray matter and whole cord level were placed on the high-resolution mFFE acquisition and transferred to the integrated APT CEST maps to calculate mean APT values for both patients and controls.

Results & Discussion: Figure 1 shows representative results from a healthy control (Fig. 1A,D) and a MS patient (Fig. 1B,E). The anatomical mFFE (Fig. 1A, B) demonstrates excellent contrast in white and gray matter in both healthy and MS patients, and distinguishes lesions in both the dorsal and ventrolateral columns of the spinal cord in the MS patient (red arrows). The CEST spectra of the whole cord (solid lines) with their respective Lorentzian fits (dashed lines) are shown in Fig. 1C. Note broader signal difference in the tails (2-4 ppm) of the CEST z-spectrum in the MS patient relative to the control, and also the peaks in the CEST spectra around 2 and 3-4ppm, which may be reflective of hydroxyl amines (glycosaminoglycans) and amide protons, respectively. The residuals from the difference of the data and fit are also plotted along the right y-axis (orange). The mean integrated values for each column in the patient and control are given in the table below and further illustrated in the calculated APT maps (Fig. 1D and 1E) overlaid on the mFFE. It should be noted that the high APT values surrounding the spinal cord indicate that this model does not accurately model CSF flow due to the long T_1 and T_2 relaxation times. The maps and reported APT values, however, spatially agree with the differences identified in the MS patient in the mFFE. Interestingly, it can be seen that compared to the relatively low-concentration APT CEST in the healthy volunteer, the calculated APT map in the MS patient shows profound tissue changes marked by increased APT concentrations at the lesion sites. These initial findings provide valuable information for characterizing lesions in MS and demonstrate the potential for APT CEST imaging in the spinal cord for diseased processes.

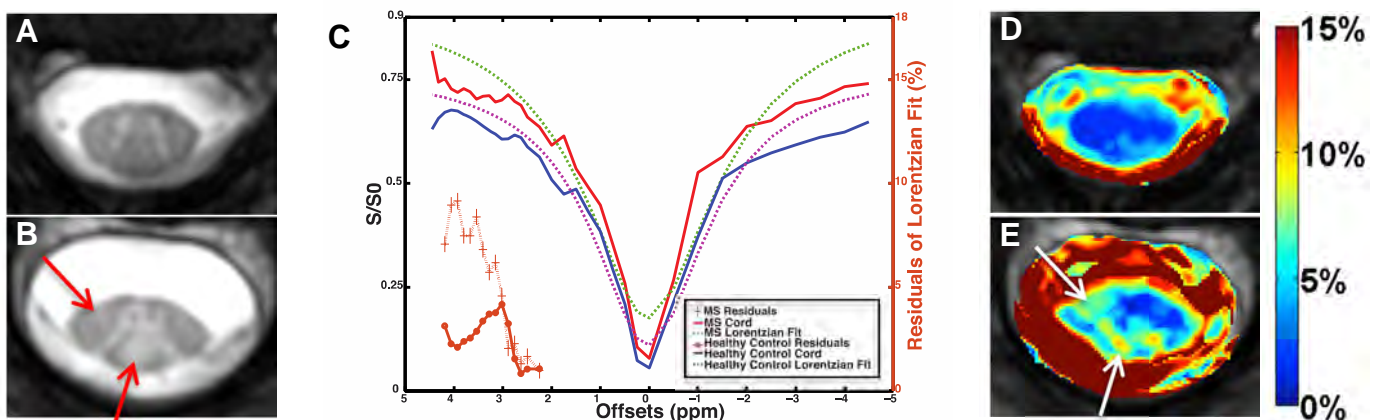


Figure 1: Comparison of CEST analysis in a representative healthy control to MS patient. A) Anatomical mFFE of a healthy cervical spine in the axial plane, B) mFFE of a MS patient, highlighting the apparent lesions with arrows in the dorsal and ventrolateral columns, C) z-spectra of the whole cord in healthy control (blue solid) and MS patient (solid red) along with their respective Lorentzian fits (dotted); the difference of the z-spectrum and fit are plotted as residuals (orange), D) APT map overlaid on mFFE of a healthy control, calculated by integrating the residuals from 3-4 ppm, E) APT map of MS patient diagnosed with lesions, demonstrating the method's sensitivity to pathology.

References: 1) Zhou, J., et al., Nat Med, 2003. **9**(8): p. 1085-1090. 2) Dula, A., et al. Proc. ISMRM 2011, #407. 3) Held, P., et al. J Neuroradiol, 2003. **30**(2): p. 83-90. 4) Jones, C.K., et al. Magn Reson Med, 2012. **67**(6): p. 1579-1589. 5) Zaiss, M., B. Schmitt, and P. Bachert, J. Magn. Reson, 2011. **211**(2): p. 149-155.

	Lateral column	Dorsal column	Gray matter	Spinal cord
Healthy	$2.69 \pm 1.01\%$	$2.76 \pm 0.91\%$	$2.43 \pm 0.93\%$	$2.90 \pm 1.31\%$
MS	$5.29 \pm 2.35\%$	$7.33 \pm 2.04\%$	$5.15 \pm 2.29\%$	$5.82 \pm 0.61\%$